Acetylacetone stimulus effect on electrorheological properties of TiO2 aggregated nanoparticles.

Alaedin Kossi, Jacques Persello, Bernard Cabane

Acetylacetone stimulus effect on electrorheological properties of TiO_2 aggregated nanoparticles

Alaedine Kossi[†], Jacques Persello[†] and Bernard Cabane[‡]

[†]LPMC, CNRS UMR 7336, Université de Nice-Sophia Antipolis, Parc Valrose 06108 Nice, France
[‡]PMMH, ESPCI, 10 rue Vauquelin, 75231 Paris, Franc

ABSTRACT

We present experimental results on electrorheological behavior under an ac electric field, and dielectric properties of colloidal suspensions composed of aggregated titanium dioxide nanoparticles dispersed in insulating PDMS silicon oil, as a function of adsorbed acetylacetone (Acac) dipolar molecules on TiO_2 surface. The results show that the elastic modulus G' of TiO_2-Acac/PDMS ER fluid decreases when the electric field frequency is increased gradually from 10 Hz to 10^4 Hz. In the range of tested electric field frequencies, we observe that the dielectric properties are given essentially by an interfacial polarization which is maximal at low frequency. At low frequency (υ=10 Hz), G' increases with the increasing Acac/TiO_2 surface coverage θ from 0 to 0.45, due to the high polarization of the particles caused by the increase of the charge carriers that move to the interface between TiO_2 particles and the insulating medium. For θ = 0.35, G' reaches 1.80 MPa which is 3.6 time greater than that of pure TiO_2/PDMS ER fluid. However, G' decreases by increasing θ beyond 0.45; in such cases, the mismatch on dielectric constant and conductivity between dispersed phase (TiO_2) and insulating medium (PDMS) begins to fall as θ increases because of the increase of Acac dipoles remaining free in PDMS. The performance of TiO_2-Acac/PDMS ER fluid at low frequency was validated by a reversibility test where elastic modulus G' increases dramatically and returns to its initial state as soon as several cycles of a switching electric field were applied between 0 and 1 kV/mm successively.

INTRODUCTION

Electrorheological (ER) fluids are made by suspending particles in a liquid dielectric constant and conductivity of which are mismatched to create dipolar particle interactions in the presence of an ac or dc electric field [1]. The ER phenomenon is related to changes in rheology of dispersions. Indeed, in response to an applied electric field, ER fluids increase their resistance to flow, and in some cases, they manifest in the conversion of fluid into solid behavior [2]. The main cause inducing this phenomenon is the polarization of particles which can be aligned in the direction of an applied electric field. For this reason, the ER effect, besides the nature of dispersed particles and insulating liquid, is sensitive to the electric field and its frequency and all additives concentration that can affect the dielectric properties of the fluid. Several authors have shown that the ER response decreases with the increasing frequency of the electric field beyond a frequency of 100 Hz [3]. Other workers have studied the effects of additives such as water, urea, or other polar molecules [4-9] on performance of an ER fluid. These studies have shown that these additives improve the ER response of ER fluids in terms of shear stress or elastic modulus.

In this study, our aim is to investigate the influences of adsorbed acetylacetone (Acac), as polar molecules, and electric field frequency, on the dielectric properties and their impacts on the ER response of titanium dioxide ER fluid, in terms of elastic modulus G' and loss modulus G". The choice of Acac is motivated by its dielectric and polarizing properties (Acac has a high dielectric constant $\varepsilon_r \approx 25.7$ and a dipole moment $\mu \approx 2.78$ D (1D = 3.33564 10^{-30} C.m)), and because its good affinity with TiO_2 surface, we expect that the adsorbed Acac can enhance the ER response of the TiO_2 ER fluids.

The system consists of aggregated nanoparticles of titanium dioxide dispersed in silicone oil. In order to control the polarization forces, the dielectric constants of the titanium dioxide particles are modified by adsorbing different Acac concentrations on titanium dioxide surface. We use a Scanning Electron Microscopy, X-Ray diffraction and small-angle neutrons scattering to characterize titanium dioxide morphology, and UV spectroscopy to determine the adsorption isotherm of Acac on titanium dioxide surface. The dielectric properties of titanium dioxide dispersed in silicone oil are measured using impedance spectroscopy. We analyze the ER response under ac electric field depending in adsorbed Acac amount onto TiO_2 surface and in electric field frequency.

EXPERIMENTAL SECTION

Synthesis of nanoporous TiO_2 powder

Nanosized TiO_2 powder was synthesized via a sol–gel method [10], using titanium tetraisopropoxide (Sigma-Aldrich, 98%, solution), 2-Propanol (Sigma-Aldrich, ACS reagent, ≥99.5%), aluminum isopropoxide (Aldrich, 99.99%), ammonium hydroxide (Sigma-Aldrich,28% NH_3 in H_2O), Acac (Sigma-Aldrich, ReagentPlus®, ≥99%), nitric acid (Sigma-Aldrich, ACS reagent, 70%), acetic acid (Sigma-Aldrich, ACS reagent, ≥99.7%) and ultrapure water (≥18 MΩ.cm) as starting materials.

In a typical procedure, titanium (IV) tetraisopropoxide (0.388 mol), was rapidly added to ultrapure water (640 ml) and then stirred for 30 min. A white precipitate formed immediately upon addition of the titanium (IV) isopropoxide. The resultant colloid was recovered by centrifugation (10,000 x g for 30 min). The centrifugation cake was added into a jacketed three-necked flask reactor equipped with a mechanical stirring containing 750 ml of an aqueous solution, of molar composition ; 0.36 M nitric acid, 1 M acetic acid and 0.05 M aluminium isopropoxide. The pH of the colloidal solution after addition of the cake was measured to be between 1 and 2.

Peptization occurred after heating the product at 80 °C for 1 h under medium stirring, whereupon the slurry became a stable sol. Then, the sol was cooled down to room temperature, and 17 M ammonium hydroxide solution was added drop wise into the TiO_2 sol under mild stirring to form a white gel. The pH of the resultant colloidal suspension was measured to be close to 7. The gel was then collected by centrifugation (10,000 x g for 30 min) and dried at 110°C over night. The powder was crushed and ground into fine powder using a mortar and pestle and was further calcined in air at 500°C for 4 h.

Characterization of the nano-porous TiO_2 particles

Electron Microscopy was performed on the CCMA EM Core Facility (University of Nice Sophia Antipolis) using a Scanning Electron Microscopy apparatus (JEOL 6700F) to characterize the TiO_2 obtained after heat treatment at 500°C. The crystal structure of the obtained TiO_2 powder was analyzed using an X-ray diffractometer (CPS120/Cu) (XRD $K_\alpha Cu$, λ=0,15406nm).

Morphological characteristics of aggregated particles can be deduced from the small angle neutron scattering [11] spectra realized on a TiO_2 heat-treated at 500°C and dispersed in silicone oil. The SANS experiments of a concentrated TiO_2/PDMS suspension are realized at the ILL institute using the D11 instrument. In a typical signal of concentrated dispersions where isotropic interactions between identical particles are considered, the average distance between the nearest neighbors is given by $r = 2\pi/q_0$ where q_0 corresponds to the maximum in scattered intensity $I_{max}(q_0)$. In the case of two-phase system, at large q vectors, the interface between particles and solvent is observed at small scale. The Porod limit can be used for a sharp interface (in the normal direction but smooth in any parallel direction) where the scattered intensity decreases as q^{-4} does at large q. the Porod limit in this case reaches a constant at large q values and is related to the specific area of particles (independently of the shape of the two phase) as [12]:

$$\lim_{q\to\infty} q^4 I_q = cste = 2\pi(\Delta\rho)^2 S/V \quad (1)$$

Where $(\Delta\rho)^2$, given in m^{-4}, is a constant related to the difference in contrast between the TiO_2 and PDMS [13], and S/V is the surface per volume unit ratio. The specific area denoted S_S (given in m^2/g) is connected to S/V through the relation:

$$S_s = \frac{1}{d^0_{TiO_2}} . S/V \quad (2)$$

where d^0_{TiO2} is the TiO_2 density. $\lim_{q\to\infty} q^4 I_q$ (q.a>10) is determined experimentally by plotting $q^4 Iq$ versus q.

For porous systems (aggregates formed from nano-particles assembling), in some cases, the two length scales: nanopores (or nano-particles) of few nanometer on one hand, and micronic grains on the other are largely separated. A typical signal may be obtained where three different regimes are observed on all samples: (I) a Porod's regime at low q values ($q < q_1$) due to the envelope of the grains, (II) a transition regime in between, and (III) a second Porod's regime at high q values ($q > q_2$) due to the inner pores of the grains [14]. Solvent PDMS is present in the inner pores and intergrain porosity. Introducing V_e as the total volume of the envelopes of the grains, σ being the total inner surface of the solid grains, and S_e as the total surface of the envelopes of the grains, one gets:

- from high-q Porod's law: $$\frac{\sigma}{V_e}(m^{-1}) = \frac{q_2^4 I(q_2)}{2\pi(\Delta\rho)^2} \quad (3)$$

- from low-q Porod's law: $$\frac{S_e}{V_e}(m^{-1}) = \frac{q_1^4 I(q_1)}{2\pi(\Delta\rho)^2} \quad (4)$$

Finally, combining the two Porod's law we obtain: $$\frac{q_2^4 I(q_2)}{q_1^4 I(q_1)} = \frac{\sigma}{S_e} \quad (5)$$

Preparation of ER fluids

In a typical procedure, several solutions of various amounts of Acac [15] in PDMS oil silicone (Dow Corning Corporation XIAMETER® PMX-200 silicone fluid, viscosity 10 cSt at 25°C) were prepared (in the range of 0 -3.215 wt%). The final ER fluids were obtained by dispersing 5 g of TiO_2 powder in 5 g of Acac silicone oil solutions by means of a Sonifier Vibra-cell (75041) ultrasonic apparatus operating at 30% amplitude for 4 min, to have a volume fraction of 0.2 of TiO_2 in PDMS. Then the ER fluid was out-gassed at room temperature and at 10^{-3} Pa for 1 h. Afterward, dry N_2 was introduced into the bowl up to a pressure of 1 atm to avoid any contamination by the humidity of the air. The ER fluids were stored in desiccators before use.

Adsorption isotherms of Acac onto TiO_2 dispersed in PDMS

Various amounts of Acac were added to TiO_2 – PDMS dispersions, and the part of Acac that had reacted with TiO_2 in each sample was determined through the depletion method: after 48 h of equilibration, the TiO_2 particles were separated through centrifugation, and the concentration of Acac in the supernatants was measured through UV spectroscopy after filtration of the samples through 0.22 µm filters.

We define surface coverage, θ, as the fraction of the adsorption sites of TiO_2 occupied by Acac molecules; at equilibrium we have:

$$\theta = \frac{\frac{m_{Acac}^{ads}}{M_{Acac}} . N_a . A°_{Acac}}{m_{TiO_2} S_{TiO_2}} \quad (6)$$

where, $A°_{Acac}$ is the area occupied by one molecule of Acac, M_{Acac} is the Acac molar mass, N_a is the Avogadro number, m_{TiO2} is the TiO_2 weight and S_{TiO2} is the TiO_2 specific area.

The experimental surface coverage can be compared with θ being calculated from the Langmuir equation [16, 17], it is given as follows:

$$\theta_{Langmuir} = \frac{b\phi_{Acac}^{équil}}{1 + b\phi_{Acac}^{équil}} \quad (7)$$

where, ϕ_{Acac}^{equil} is the volume fraction of unadsorbed Acac in equilibrium with the dispersion. b is adsorption/desorption equilibrium constant of Acac on TiO_2, it is given by following:

$$b = \left(\frac{h^2}{2\pi . m_{Acac}^{\circ} . kT} \right)^{3/2} \frac{3}{4\pi . a_{acac}^3} e^{-\varepsilon / kT} \quad (8)$$

where : $m_{Acac}^{\circ} = \rho_{Acac} \frac{4\pi}{3} a_{Acac}^3 \approx 2{,}156.10^{-25} Kg$ is the mass of one Acac molecule, h is the Planck constant, k is the Boltzmann constant, T≈298K is the temperature and ε is the interaction energy between TiO_2 and Acac.

Electrorheological measurements

The dynamic properties of electrorheological fluids were measured by means of a Rheometrics Dynamic Analyzer II (RDA II, Rheometrics, Inc., NJ) in time sweeps mode. These measures consist of applying an alternating electric field (Trek Model 609E-5 High Voltage amplifier and Hameg function generator HM 8030-5 on a sample placed between two parallel plane-plane geometry electrodes and measuring moduli as a function of time until a stationary state is reached. The diameter of plane electrode was 25 mm, and the gap between electrodes was 1 mm. The moduli are measured at low shear strains, where dynamic properties are independent of shear strain amplitude. The mobile electrode (upper electrode) applies an oscillatory shear strain with γ_m=0.2% of amplitude, at constant temperature of 25°C and with an angular velocity of ω=100 rad/s. An ammeter (TENMA 72-7735 Multimeter) is used to measure the electrical current passing through the sample during rheological measurements under applied electric field.

Complex relative permittivity measurement

We use an HP 4192A LF impedance analyzer to measure the dielectric properties of the prepared ER fluids. The frequency range of the applied alternating field was between 5Hz and 1MHz. The dielectric cell consists of parallel stainless steel electrodes separated by a distance *l* that we can change. The electric circuit can be represented by a parallel equivalent schema (Fig. 1) where we consider the contribution, in total measured impedance (G, C), an impedance (G_k, C_k) due to the sample polarization, a stray impedance (G_e, C_e) due to electrode polarization, and a residual capacitance (C_r) due to the field lines that are not located in the sample. We can determine G_e and C_e by measuring the total impedances at different electrode distances for a given frequency. To calculate C_r, we measure capacitance C of an empty cell as a function of the inverse of distance between electrodes, C is given by:

$$C = C_R + \frac{\varepsilon_0 S^*}{l} \quad (9)$$

where ε_0 is the vacuum permittivity, S^* is the electrode effective surface, and *l* is the distance between parallel electrodes.

Henceforth, once these corrections are made, we can determine the samples impedance (G_k, C_k) [18, 19] that can be related to the complex relative permittivity by:

$$\varepsilon'_{rk} = \frac{C_k}{C_0} \text{ and } \varepsilon''_{rk} = \frac{G_k}{\omega C_0} \quad (10)$$

where C_0 is the vacuum capacitance, and ω is the ac electric field angular frequency.

Experimental measurements of (ε_{rk}') and (ε_{rk}'') obtained from Eq. (10) are fitted by using the Maxwell-Wagner equations [20], yielding ε_{rk}' and ε_{rk}'' as:

$$\varepsilon_{rk}' = \frac{(\varepsilon_{rk}')_S - (\varepsilon_{rk}')_\infty}{1+\omega^2\tau} + (\varepsilon_{rk}')_\infty \quad (11)$$

$$\varepsilon_{rk}'' = \frac{(\varepsilon_{rk}')_S - (\varepsilon_{rk}')_\infty}{1+\omega^2\tau^2}\omega\tau + \frac{\sigma_k'}{\omega\varepsilon_0} \quad (12)$$

where, $(\varepsilon_{rk}')_s$ and $(\varepsilon_{rk}')_\infty$ are, respectively, the static value (when ω tends to 0) and the optic value (when ω tends to ∞) of relative permittivity, σ_k' is the sample conductivity, and τ is the relaxation time of the dielectric function.

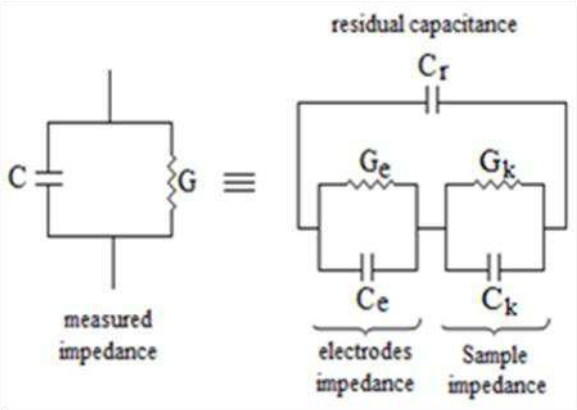

Fig. 1: *Schematic representation of the equivalent circuit for measuring dielectric properties.*

RESULTS AND DISCUSSION

Morphology and structure of TiO_2 aggregated nanoparticles

SEM performed on TiO_2 after heat treatment at 500 °C (Fig. 2) shows nanosized particles (between 10 and 20nm) highly aggregated forming a porous system. The x-ray spectra (Fig. 3) show that the obtained TiO_2 powder had an anatase crystalline structure. The density of TiO_2 was determined using a standard flask pycnometer of 5 cm^3, and we found a value of 3.84g/cm^3 that is close to the TiO_2 anatase density (3.89g/cm^3).

The SANS curve giving the scattered intensity Iq versus wave vector q is shown in (Fig. 4a). A maximum of the scattered intensity is observed for an intermediate value of wave vector ($q(Imax) \approx 3.56.10^{-1} nm^{-1}$), which characterizes the average interparticle distance $r=2\pi/q_{max}$, in our case (adhesive particles heat treated at 500°C) we can confuse r with the average size of the nanoparticles. We obtain the average radius of the TiO_2 nanoparticles about a ≈ 8.8nm which is in the same range as that observed in the SEM picture. From the Porod plot (Fig. 4b) at very high value of q (where Iq is proportional to q^{-4} and q.a>10), we can use the Porod limit (Eqs. (1) and (2)) to calculate the specific area of TiO_2 particles. We obtain a specific area $S_s \approx 117 m^2/g$. (Fig. 4b) shows also two porod's regimes: the first for $q < q_1 = 0.09\ nm^{-1}$ which characterizes the interface of the envelope of the grains S_e, the second for $q > q_2 = 0.53\ nm^{-1}$ which can be attributed to the surface of inner porous structure σ. Using Eq. (5), a high ratio (σ / S_e) = 263 was obtained indicating that the porosity of the system is dominated by inner nanoporous structure.

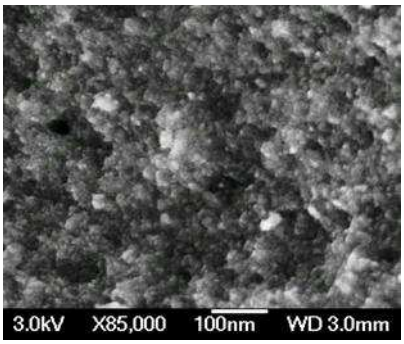

Fig. 2: *SEM picture of TiO_2 particles calcined at 500°C/4h.*

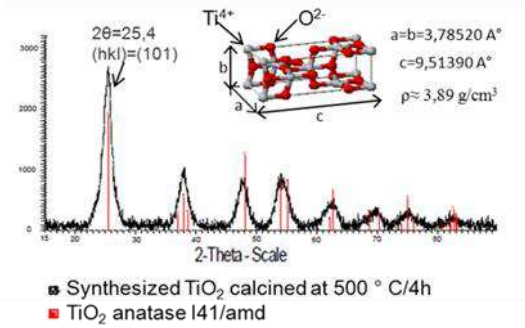

Fig. 3: *X-Ray spectra (XRD $K_\alpha Cu$, λ=0,15406nm) performed on TiO_2 particles after calcination at 500°C/4h, black line for synthesized TiO_2 calcined at 500°C/4h and red lines for pure TiO_2 anatase I41amd.*

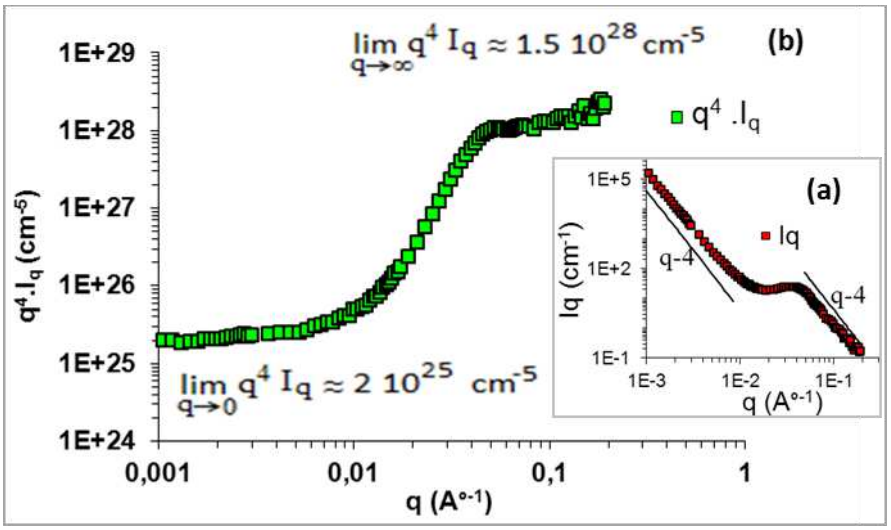

Fig. 4: *The SANS spectra of the heat treated TiO_2 dispersed in PDMS:* ***(a)*** *giving the scattered intensity Iq (cm^{-1}) versus wave vector q ($A^{\circ -1}$);* ***(b)*** *giving the Porod representation $q^{-4}Iq$ (cm^{-5}) as a function of wave vector q ($A^{\circ -1}$)*

Influences of electric field and its frequency on electrorheological properties

The elastic modulus G' and loss modulus G" for TiO_2-Acac/PDMS ER fluid measured in the applied electric field range 0-4 kV/mm versus electric field frequency are shown in (Fig. 5a, b).

We note that G' and G" decrease with the increasing electric field frequency, and this occurs whatever be the applied electric field supportable by the sample. We also note that the increase in electric field frequency is accompanied by a decrease in the maximum of electric field E_{max} supportable by the apparatus. This limitation of applied electric field is due to the appearance of an electric current density which is insignificant at low frequency, but becomes increasingly important as soon as the frequency increases.

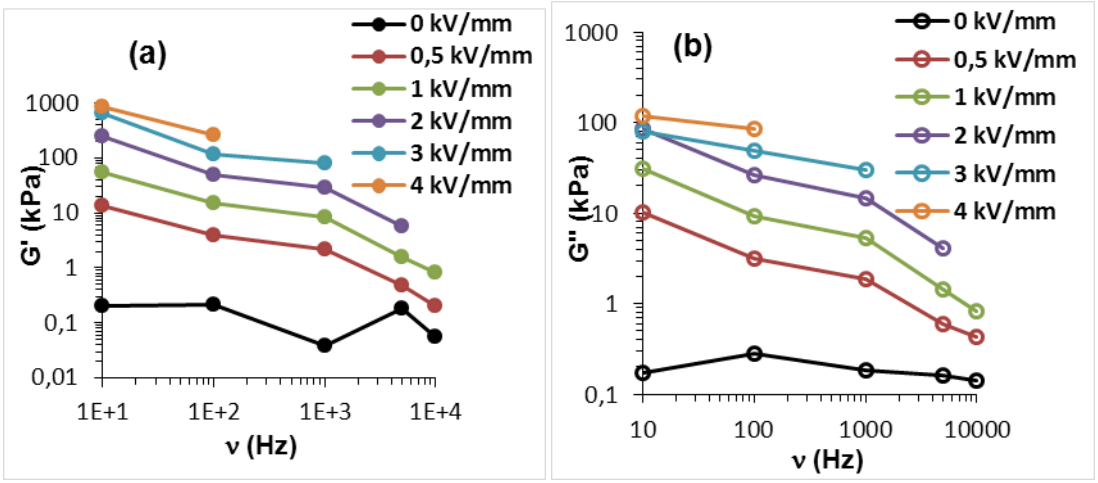

Fig. 5: *Elastic modulus G'* ***(a)****, and loss modulus G"* ***(b)*** *versus electric field frequency at various applied electric fields of TiO_2-Acac/PDMS ER fluid.*

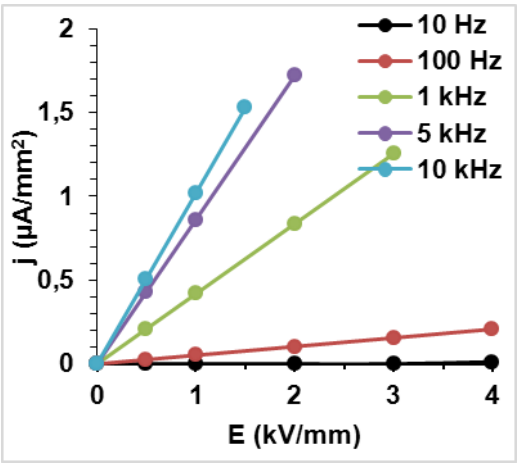

Fig. 6: *Variation of the current density with respect to the applied ac electric field at various frequencies.*

(Figure 6) illustrates this situation where at low frequency (υ=10Hz) E_{max} can be up to 4kV/mm, and the electric current density in the sample is very low ($j_{(Emax)}$ =0.01µA/mm^2), while at high frequency (υ=10kHz) E_{max} is limited to 1.5kV/mm ($j_{(Emax)}$≈1.53µA/mm^2); beyond this limit, the measurement is interrupted because of the high conduction in the sample.

Dielectric properties of TiO_2-Acac/PDMS ER fluid

To understand the link between the ER behavior depending on the frequency and the dielectric properties, we have made measurements of the complex impedance versus frequency for TiO_2-Acac/PDMS ER fluid. Figure 7 shows the experimental and the calculated results (using the Maxwell-Wagner equations) of the real part of relative permittivity (ε_r') (Fig. 7a) and imaginary part ε_r'' of relative permittivity (Fig. 7b) versus frequency (ν) for TiO_2-Acac/PDMS ER fluid.

We observe that at low frequency we have a macroscopic polarization due essentially to an interfacial polarization where its contribution to dielectric constant is maximal because the motions of the charge carriers that are accumulated at the interface between TiO_2 and insulating medium. At high frequency, the electric field alternates so fast such that the interfacial polarization cannot increase, and there is no contribution to the dielectric constant. However, between these two limits (low and high frequency), at intermediate frequencies, the interfacial polarization begins to lag behind the electric field causing dissipative losses [21]. This energy dissipation is maximal when the loss tangent $tg\delta = \varepsilon_r''/\varepsilon_r'$ reaches a maximum value at an angular frequency ω_m that can be related to the characteristic relaxation time τ as follows:

$$\tau = \frac{1}{2\pi \nu_m} = \frac{1}{\omega_m} \quad (13)$$

For TiO_2-Acac/PDMS ER fluid, we found $\tau \approx 7.10^{-5}$s, corresponding to υ_m about 2.3 kHz. The frequency below υ_m determines the range in which charge carriers are mobile on long distances. At frequency above υ_m, the charge carriers are confined to potential wells being mobile on short distance.

The influence of frequency on the polarization in terms of dielectric losses caused by the energy dissipation in the sample may explain the ER behavior where the elastic modulus G' decreases as the electric field frequency increases between 10 Hz and 10 kHz.

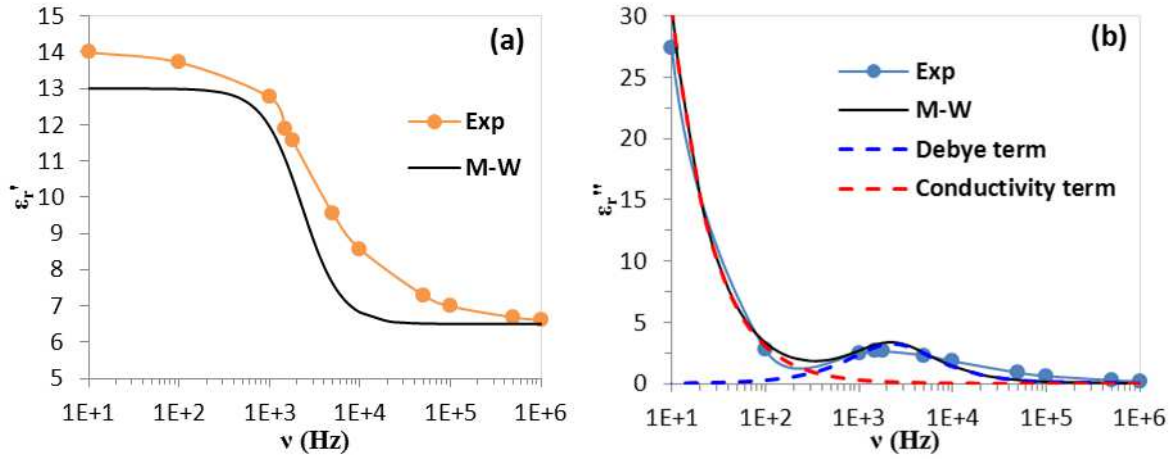

Figure 7: *TiO_2-Acac/PDMS ER fluid dielectric properties,* ***(a)*** *real part of relative permittivity ε_r' versus frequency;* ***(b)*** *imaginary part of relative permittivity ε_r'' versus frequency compared to the calculated ε_r' and ε_r'' using Maxwell-Wagner equations (M-W).*

The ER results and dielectric characterization clearly show that ER effect is optimal at low frequency. The following ER experiences will be investigated with a fixed applied electric field E = 1kV/mm and with a frequency υ=10Hz to have an ER effect satisfactory without the occurrence of a current strong enough, energy consumer and disruptive of ER measurement.

Influence of the added Acac on electrorheological properties

To quantify the role of Acac on the TiO_2/PDMS ER properties, the Acac onto TiO_2 surface adsorption isotherm is shown in (Fig. 8). The experimental results giving the surface coverage (θ) as a function of the volume fraction of free Acac in equilibrium with the dispersion are compared to those calculated from Langmuir equation. The best fit between experiment and Langmuir equation was obtained using an interaction energy ε=-8.85 10^{-20}J (-21.5kT) and an adsorption/desorption equilibrium constant b=6.88 10^3 where the adsorption of Acac onto TiO_2 surface reaches a plateau for $\theta \approx 0.90$ corresponding to a maximum adsorption about 2Acac/nm^2. However, a discrepancy was observed between the calculated and the experimental results for $\theta > 0.65$ suggesting that Acac is adsorbed onto TiO_2 surface in a multilayer manner. The results show also that the Acac adsorption onto TiO_2 surface is virtually total for $\theta \leq 0.45$, while beyond this limit, the Acac remaining free in PDMS becomes significant and increases with surface coverage θ.

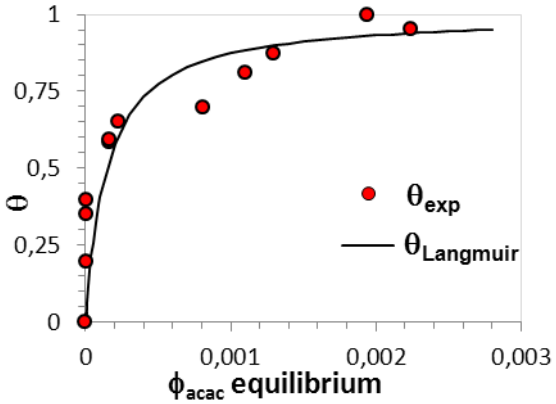

Fig. 8: *Acac/TiO2 in PDMS adsorption isotherm giving surface coverage ϑ versus the free Acac volume fraction at equilibrium in PDMS compared to that calculated trough Langmuir equation.*

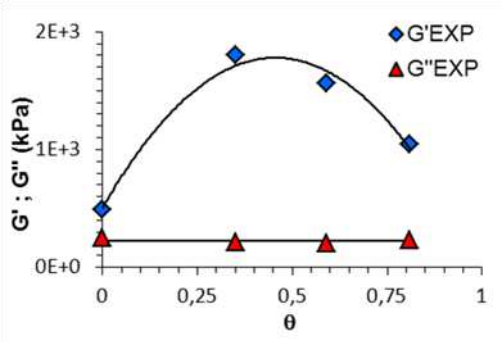

Fig. 9: *Elastic modulus G' and loss modulus G" versus Acac/TiO_2 surface coverage ϑ. The characteristics of the applied electric field and the shear strain are, respectively: E=1kV/mm v_E=10Hz γ_m = 0.2 % and ω_γ = 100 rad/s.*

According to the Acac onto TiO_2 surface adsorption isotherm, four ER fluids samples were investigated where different situations are represented: pure TiO_2/PDMS ER fluid (θ=0), total Acac adsorption onto TiO_2 surface (θ=0.35), and two samples with partial Acac adsorption onto TiO_2 surface, respectively: θ=0.59 and θ=0.81. In all samples, Φ_V (TiO_2/PDMS) = 0.2. We carried out measurements of elastic modulus G' and loss modulus G" on the four samples prepared above. Figure 9 represents the experimental results of G' and G" obtained from the various samples prepared according to surface coverage rate, θ, of Acac adsorbed onto TiO_2.

Figure 9 shows that the intrinsic ER properties of TiO_2 ER fluid (without adding Acac θ=0) are very correct and reach an elastic modulus G' of about 500kPa and G" of about 225kPa with an applied ac electric field of 1kV/mm and 10Hz of frequency. It also shows that, for the same electric field and dynamic shear rheology conditions, the increase of adsorbed Acac onto TiO_2 surface leads to an increase of G' until it reaches a maximum G'_{max}≈1,80MPa which is 3.6 times greater than that for pure TiO_2/PDMS ER fluid. This maximum corresponds to the surface coverage θ≈0.45 (about 1Acac/nm^2). Beyond this limit G' decreases. As observed in (Fig.8), we can attribute this behavior to the TiO_2/Acac/PDMS adsorption equilibrium that may affect the dielectric properties of ER fluid. Indeed for θ ≤ 0.45 the amount of Acac, remaining free in the dispersing medium is negligible. Hence, the increase in surface coverage, from 0 to 0.45, results in an increase of interaction energy between particles due to the improvement of the interfacial polarization of the particles, by increasing the number of charge carriers that move to the interface between the TiO_2 particles and the insulating

medium. While for θ > 0.45, the mismatch on dielectric constant and conductivity between dispersed phase (TiO_2) and insulating medium (PDMS) begins to fall as θ increases due to the increase of Acac dipoles remaining free in PDMS. Therefore, the part of the interaction energy that is dissipated through the insulating medium becomes significant leading to a decrease in G'. Figure 9 shows also, that loss modulus G" remains virtually constant over the entire θ range. This means that by adsorbing Acac dipoles on TiO_2 surface, only the elasticity (dependence of G' on the interaction energy) was influenced by adding Acac, and in this dynamic oscillation conditions (γ=0.2% and ω_γ=100rad/s) there are no restructuring (no change on viscosity) and the deformation of the aligned structures developed by the applied electric field that still remains unchanged.

To validate the TiO_2-Acac/PDMS ER performance, we carried out measurements of elastic modulus (Fig. 10) where the applied ac electric field (υ=10Hz) switches between 0 and 1kV/mm successively. We find that the elastic modulus G' increases dramatically with the electric field and returns to its initial state as soon as the electric field is removed, and this is reproducible over several cycles where E switches between 0 and 1kV/mm successively. This result confirm that at low frequency (υ=10Hz) the studied systems are reversible.

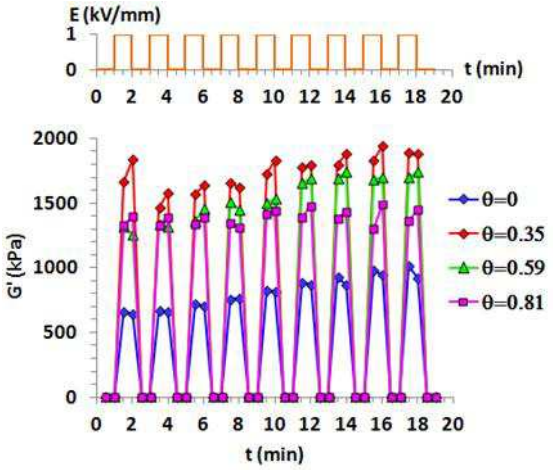

Fig. 10: *Reversibility test; Elastic modulus G' versus the switching electric field between 0 and 1kV/mm (υ=10Hz) successively, for different amount of Acac adsorbed on TiO_2 surface.*

CONCLUSION

ER fluids have been prepared by suspending porous aggregates of TiO_2 nanoparticles in PDMS silicone oil. The porous nature of TiO_2 aggregates is exploited to adsorb dipolar molecules of Acac onto TiO_2 surface. The TiO_2 volume fraction Φ in PDMS was about 0.2. Electrorheological properties of ER fluids are investigated under ac electric field. The results show that the elastic modulus G' of TiO_2-Acac/PDMS ER fluid decreases with the gradually increasing electric field frequency from 10 to 10^4Hz. In the range of the tested electric field frequencies, we observe that the dielectric properties are given essentially by an interfacial polarization which is maximal at low frequency. We studied the influence of the adsorbed Acac in terms of surface coverage θ on ER response of TiO_2 ER fluids, the applied ac electric field, and its frequency are, respectively: E=1kV/mm and υ=10Hz. The result shows that G' increases with the increasing surface coverage θ, from 0 to 0.45, because of the high polarization of the particles caused by the increase of the charge carriers that move to the interface

between TiO_2 particles and the insulating medium. For θ = 0.35, G' reaches 1.80 MPa which is 3.6 times greater than that of pure TiO_2/PDMS ER fluid. However, G' decreases by increasing θ beyond 0.45; in such cases, the mismatch on dielectric constant and conductivity between dispersed phase (TiO_2) and insulating medium (PDMS) begins to fall as θ increases because of the increase of Acac dipoles remaining free in PDMS. The performance of TiO_2-Acac/PDMS ER fluid at low frequency was validated by a reversibility test where elastic modulus G' increases dramatically and returns to its initial state as soon as several cycles of a switching electric field were applied between 0 and 1 kV/mm successively.

Acknowledgments

The authors wish to thank Ralph Schweins from the Institut Laue-Langevin (ILL) for technical assistance in SANS experiments. The authors also gratefully acknowledge the financial support from the ANR CNRS.

References

[1] W. M. Winslow, *Induced fibration of suspensions*, J. Appl. Phys. **1949**, 20, 1137-1140

[2] H. Block, J. P. Kelly, *Electro-rheology*, J. Phys. D: Appl. Phys. **1988**, 21, 1661-1677

[3] Hongru Ma, Weijia Wen, Wing Yim Tam and Ping Sheng, *Frequency dependent electrorheological properties: origin and bounds*, Phys. Rev. Lett. 1996, 77, 2499-2502

[4] F. Ikazaki, A. Kawai, K. Uchida, T. Kawakami, K. Edamura, K. Sakurai, H. Anzai and Y. Asako, *Mechanisms of electrorheology: the effect of the dielectric property*, J. Phys. D: Appl. Phys. **1998**, 31, 336-347

[5] W. Wen, X. Huang, S. Yang, K. Lu and Ping Sheng, *The giant electrorheological effect in suspensions of nanoparticles*, Nature Materials, **2003**, 2, 727-730

[6] Lu et al. United States Patent, US 7, 981, 315, B2 **2011**

[7] Min S.Cho, Hyoung J. Choi and Wha-Seung Ahn, *Enhanced electrorheology of conducting polyaniline confined in MCM-41 channels*, Langmuir, **2004**, 20, 202-207

[8] Ying Dan Liu and Hyoung Jin Choi, *Electrorheological fluids: smart soft matter and characteristics*, Soft Matter, **2012**, 8, 11961-11978

[9] Ying Dan Liu, Fei Fei Fang and Hyoung Jin Choi, *Silica nanoparticle decorated polyaniline nanofiber and its electrorheological respons*e, Soft Matter, **2011**, 7, 2782-2789

[10] S. Music`, M. Gotic`, M. Ivanda et al, *Chemical and microstructural properties of TiO_2 synthesized by sol-gel procedure*, Science and Engineering, **1997**, B 47, 33-40

[11] A. Guinier, Ann. Phys. Paris, **1939**, 12, 161-237

[12] D. Marchal, C. Bourdillon and B. Demé, Langmuir, *Small-angle neutron scattering by highly oriented hybrid bilayer membranes confined in anisotropic porous alumina*, **2001**, 17, 8313-8320

[13] J. Schweizer, *Neutrons et matériaux: introduction*, J. Phys. IV (France), **2003**, 103

[14] L. Girard, M. Arab, O. Spalla, *Time resolved alteration process of oxide glasses*, Journal of Colloid and Interface Science, **2008**, 319, 214-225

[15] G. Buemi, C. Gandolfo, *Malondialdehyde and acetylacetone. An AM1 study of their molecular structures and keto–enol tautomerism*, J. Chem. Soc., Faraday Trans. 2, **1989**, 85 (3), 215-227

[16] I. Langmuir, *The constitution and fundamental properties of solids and liquids*, JACS, **1917**, 39, 1848-1906

[17] Y. Liu, J. I. Dadap, D. Zimdars, and K. B. Eisenthal, *Study of interfacial charge-transfer complex on TiO_2 particles in aqueous suspension by second-harmonic generation*, J. Phys. Chem. B, **1999**, 103, 2480-2486

[18] Z. Mimouni, Ph.D Thesis, University of Nice Sophia-Antipolis, France (**1990**)

[19] Q. Wu, B. Yuan Zhao, C. Fang and K. Ao Hu, *An enhanced polarization mechanism for the metal cations modified amorphous TiO_2 based electrorheological materials*, Eur. Phys. J. E, **2005**, 17, 63-67

[20] L. M. Dudley, S. Bialkowski, D. Or and C. Junkermeier, *Low frequency impedance behavior of montmorillonite suspensions: Polarization mechanisms in the low frequency domain*, Soil Sci. Soc. Am. J. **2003**, 67, 518-526

[21] S. Orlowska, Ph.D Thesis, Ecole Centrale de Lyon, France (**2003**).